

Liposomes Physically Coated with Peptides: Preparation and Characterization

Cuicui Su,[†] Yuqiong Xia,[‡] Jianbo Sun,[†] Nan Wang,[†] Lin Zhu,[†] Tao Chen,[§] Yanyi Huang,[§] and Dehai Liang^{*,†}

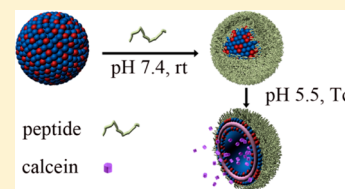
[†]Beijing National Laboratory for Molecular Sciences and the Key Laboratory of Polymer Chemistry and Physics of Ministry of Education, College of Chemistry and Molecular Engineering, Peking University, Beijing 100871, China

[‡]School of Life Sciences and Technology, Xidian University, Xi'an, Shanxi 710126, China

[§]Biodynamic Optical Imaging Center (BIOPIC), Peking University, Beijing 100871, China

Supporting Information

ABSTRACT: Physically coating liposomes with peptides of desirable functions is an economic, versatile, and less time-consuming approach to prepare drug delivery vehicles. In this work, we designed three peptides—Ac-WWKKKGGNNN-NH₂ (W2K3), Ac-WWR-RRGGNNN-NH₂ (W2R3), Ac-WWGGGGGNNN-NH₂ (W2G3)—and studied their coating ability on negatively charged liposomes. It was found that the coating was mainly driven by the electrostatic interaction between the peptides' cationic side groups and the acidic lipids, which also mediated the “anchoring” of Trp residuals in the interfacial region of lipid bilayers. At the same conditions, the amount of the coated W2R3 was more than that of W2K3, but the stability of the liposome coated with W2R3 was deteriorated. This was caused by the delocalized charge of the guanidinium group of arginine. The coating of the peptide rendered the liposome pH-responsive behavior but did not prominently change the phase transition temperature. The liposome coated with peptides displayed appropriate pH/temperature dual responsive characteristics and was able to release the content in a controlled manner.



1. INTRODUCTION

As a potential pharmaceutical carrier of choice for numerous practical applications, liposomes have moved a long way in the transition from the laboratory to the clinic.^{1–3} To improve the robustness of the bilayer and to tune the liposomal drug release rate, polymers, such as polysaccharides and polypeptides, have been used to create a capsule wall over the liposomal surface.^{4–7} These polymer-coated liposomes have been used to create organic–inorganic hybrid nanocapsules⁸ and free-standing bioscaffold.⁹ The stimulus-sensitive liposomes, which were capable of releasing their contents in response to small changes in pH, were also developed.^{10,11} Such pH-responsive liposomes promoted the delivery of drugs (or genes) to cytosolic or nuclear targets, as the pH values were different in various tissues and cellular compartments.^{12–15}

Liposome is also treated as a model structure of cells membrane. Actually, many cellular processes are controlled by protein–protein interaction,¹⁶ and more than 50% of currently available drugs are targeted toward membrane proteins.¹⁷ In the nervous system, message regulation involves the regulation of membrane proteins in distinct types of secretory vesicles.^{18,19} The integration of liposome and peptides, as a mimic of cell membrane, combines the vesicle structure of liposome and the functions of peptides, yielding many attractive features.²⁰ It has been reported that the stearylation of cell-penetrating peptides (CPPs) oligoarginine facilitates the “programmed packaging” of genes into liposomes. A multifunctional envelope-type nano-device (MEND) modified with octaarginine was generated,

which showed high transfection efficiency.^{21,22} When pH-sensitive fusogenic peptide (GALA)²³ was anchored on the liposomal surfaces, the cytosol release was promoted.²⁴ These formulations relied on the terminal modification of peptides through the introduction of hydrophobic insertion chains. The physical absorption of peptide on the liposome surface or insertion in the bilayer, which is simpler, versatile, and less time-consuming, offers an alternative approach to integrate peptide with liposome. This is also the approach taken by many membrane proteins to bind the cell. However, the physical coating of liposomes by artificially designed peptides is rarely reported in the literature.

Herein, we designed a serial of peptides suitable for coating on the liposome surface. The sequences of the peptides are Ac-WWKKKGGNNN-NH₂ (W2K3), Ac-WWR-RRGGNNN-NH₂ (W2R3), and Ac-WWGGGGGNNN-NH₂ (W2G3). It has been proposed that, of all the 20 amino acids, tryptophan (Trp, W) has the highest affinity in the membrane–water interface.²⁵ Its side chain acts as an interfacial anchor in that the indole ring resists displacement to a deeper or shallower membrane location for an energetically favorable interaction.^{26–29} Moreover, Trp residue is a fluorophore, and its fluorescence emission spectra are very sensitive to environmental changes.^{30,31} It can act as an indicator for the

Received: April 4, 2014

Revised: May 14, 2014

Published: May 14, 2014

interactions between peptides and liposomes. Two Trp residues were employed as the C-terminal of each peptide. A short sequence of positively charged amino acids, either K or R, was selected next to the two Trp residues. The electrostatic interaction was strong and long ranged. It would facilitate the binding of peptides with negatively charged liposomes. The liposome coated with positively charged peptides was also expected to construct unique functional gene carrier.³² To test the capacity of the electrostatic interaction, a peptide without K or R, named W2G3, was designed as the control. A spacer served by two glycine (G) residues was added next to the positively charged amino acids. Glycine is an achiral amino acid with a minimal side chain of only one hydrogen atom. It can fit in either hydrophilic or hydrophobic environment, eliminating the formation of secondary structures or extra interactions. The N-terminal of each peptide was composed of three asparagine (N) residues. N3 was hydrophilic, and it was able to prevent interparticle aggregation. It can also be easily changed to some other functional sequences to expand the capacity of the peptide. The liposome was formed by 1,2-dipalmitoyl-*sn*-glycero-3-phosphocholine (DPPC) and 1,2-dipalmitoyl-*sn*-glycero-3-phospho-(1'-*rac*-glycerol) (DPPG) at varying molar ratio. DPPC and DPPG have the same melting points, which is ~ 41 °C.³³ Lateral segregation of lipid, which makes the coating of peptides more complicated, did not occur at the studied temperature range from 25 to 50 °C. This work focused on the coating capacity of peptides on liposomes and the effect of the coated peptide on the properties of liposomes.

2. MATERIALS AND METHODS

2.1. Materials and Sample Preparation. The peptides W2K3, W2R3, and W2G3 with >98% purity were purchased from GL Biochem (Shanghai) Ltd. (Shanghai, China). Dry powder of 1,2-dipalmitoyl-*sn*-glycero-3-phosphocholine (DPPC) and chloroform solution of 1,2-dipalmitoyl-*sn*-glycero-3-phospho-(1'-*rac*-glycerol) (DPPG, sodium salt) were purchased from Avanti Polar Lipids, Inc. Hepes was purchased from Sino-American Biotechnology Co., Ltd. Triton-X100 (98%) was purchased from Xilong Chemical Inc. (China). Milli-Q water (18.2 MW·cm) was used in all the experiments. All the vials were carefully washed and sterilized.

2.2. Liposome Preparations. The large unilamellar vesicles (LUV) formed by DPPC and DPPG were prepared by the lipid film method, followed by several cycles of extrusion. Briefly, a chloroform solution of the lipid mixture with desired composition was added to a 50 mL pyriform flask together with some Teflon beads. The solvent was removed by a rotary evaporator at 50 °C. The formed thin film was further dried under vacuum overnight. The dry film was then hydrated with HB buffer (pH 7.4, 20 mM Hepes, 0.1 mM EDTA) or HBS buffer (pH 7.4, 20 mM Hepes, 0.1 mM EDTA, 150 mM NaCl) at 50 °C for 1 h by a rotary evaporator (no vacuum). Occasional vortex for 10 s was conducted during the hydration process. The resulting suspension was then pushed through a polycarbonate membrane with a pore diameter of 100 nm at 50 °C for 21 times using a mini-extruder (Avanti Polar Lipids, Inc.). Liposomes encapsulating calcein were prepared by following above procedures but using 80 mM calcein in water as the hydration solution. The free calcein molecules were removed by gel filtration on a Sepharose CL-4B column equilibrated in HBS. The final concentration of liposome was determined by modified Bartlett method.³⁴

2.3. Laser Light Scattering (LLS). A commercialized spectrometer from Brookhaven Instruments Corporation (BI-200SM Goniometer, Holtsville, NY) was used to perform both static light scattering (SLS) and dynamic light scattering (DLS) over a scattering angular range of 20°–120°. A vertically polarized, 100 mW solid-state laser (GXC-III, CNI, Changchun, China) operating at 633 nm was used as the light source, and a BI-TurboCo digital correlator (Brookhaven

Instruments Corp.) was used to collect and process data. In SLS, for a very dilute solution, the weight-averaged molar mass (M_w) and the root mean-square radius of gyration (R_g) are obtained on the basis of

$$HC/R_w(\theta) = (1/M_w)[1 + (1/3)R_g^2 q^2] + 2A_2C \quad (1)$$

where $H = 4\pi^2 n^2 (dn/dC)^2 / (N_A \lambda^4)$ and $q = 4\pi n / \lambda \sin(\theta/2)$ with N_A , n , dn/dC , and λ being Avogadro's number, the solvent refractive index, the specific refractive index increment, and the wavelength of light in a vacuum, respectively. The dn/dC values of peptide and liposome are very close, both are ~ 0.154 .³⁵ Since the scattered intensity from the peptide is negligible compared with that from the liposome, and the weight ratio of peptide coated on the liposome is less than 10 wt % in all the studied conditions, the concentration of pure liposome is used to calculate the size and molecular weight.

In DLS, the intensity–intensity time correlation function $G^{(2)}(\tau)$ in the self-beating mode was measured. A Laplace inversion program, CONTIN, was used to process the data to obtain the line width distribution and diffusion coefficient. The diffusion coefficient D can be further converted into the hydrodynamic radius R_h by using the Stokes–Einstein equation

$$D = k_B T / 6\pi\eta R_h \quad (2)$$

where k_B , T , and η are the Boltzmann constant, the absolute temperature, and the viscosity of the solvent, respectively. For each sample, we measure the correlation functions at five angles covering 30°–90°. Only the CONTIN analysis at 30° or 90° is shown if the results are similar. But the calculation on hydrodynamic radius ($R_{h,app}$) is based on the extrapolation to zero angle.

The aqueous solutions of peptides and liposomes were filtered through 0.45 μm filters (Sartorius stedim Biotech, Goettingen, Germany) to remove dust. The $+/-$ charge ratio of peptides to liposomes was denoted as $\rho_{p/l}$. To calculate the coating amounts of peptides, liposomes were added to peptides at 25 °C instantly. This time point was set as t_0 . The mixture was vortexed at 1200 rpm for 20 s and then monitored by laser light scattering.

To measure the pH sensitivity of liposomes coated with peptides, 60 μL of calcein-loaded liposomes at 500 μM was added to 100 μL peptide solutions at 40 μM ($\rho_{p/l} = 1$). The mixture was then vortexed at 1200 rpm for 3 min, followed by incubating at 37 °C for 15 min. The mixed solutions was then heated to 50 °C and stayed for 30 min. After being cooled to 37 °C, the mixed solution (50 μL) was evenly distributed into the buffers (2.0 mL) at varying pHs and monitored by laser light scattering at 37 °C for a week.

2.4. Zeta Potential Analysis. Electrophoretic mobility was measured using a zeta potential analyzer (ZetaPALS, Brookhaven Instruments, Holtsville, NY). Each sample was measured three times. The zeta potential ξ was calculated using the Smoulokowski model

$$\xi = \mu\eta/\epsilon \quad (3)$$

where μ is the electrophoretic mobility ($\text{m}^2 \mu\text{s}^{-1} \text{V}^{-1}$), ϵ is the dielectric constant, and η is the viscosity of solvent.

2.5. Transmission Electron Microscopy (TEM). 10 μL of the sample was applied to a copper grid covered with a carbon film support (T10023, Beijing Xinxing Braim Technology Co., Ltd.) for approximately 30 s. The excess sample solution was removed by filter paper. A drop of 1.0% phosphotungstic acid was then placed on the grid, and the excess stain was wicked away 30 s later. The samples were viewed on a H-9000NAR transmission electron microscope after dried.

2.6. Controlled Release of Calcein. 30 μL of calcein-loaded liposomes at 500 μM was added to 50 μL of peptide solutions at 40 μM ($\rho_{p/l} = 1$). The mixture was then vortexed at 1200 rpm for 3 min. The mixed solution containing coated liposomes (50 μL) was evenly distributed into the buffers (2.0 mL) at varying pHs. After being incubated at 37 °C for 5 min, each sample was heated to 50 °C at a heating rate of 0.1 °C/min and then cooled to 37 °C at 0.2 °C/min. After the heating and cooling cycle, Triton X-100 was added to release all the calcein from the liposome. The released calcein was determined by measuring the fluorescence at $\lambda_{ex} = 490$ and $\lambda_{em} = 520$ nm. The percentage of calcein leakage was calculated according to the equation

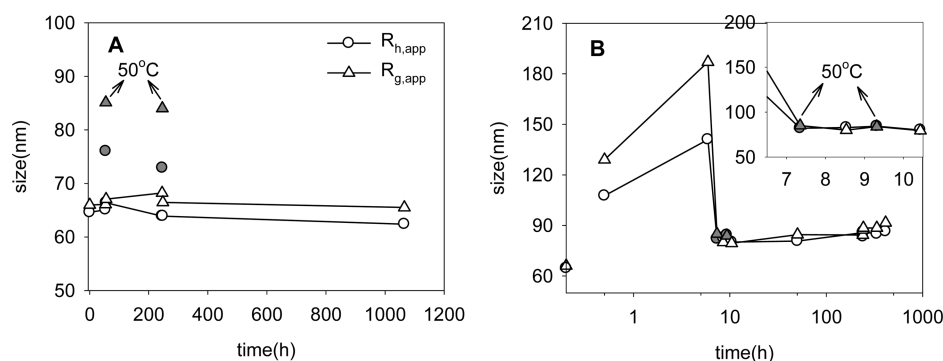


Figure 1. Time dependence of the sizes of DPPC/DPPG liposomes (60:40 m/m ratio) (A) before and (B) after added into W2K3 ($\rho_{p/l} = 20$) in HB at different time points. Temperature: 25 °C. The filled symbols show the results at 50 °C. The inset magnifies the data in the 7–10 h range.

$$F = (I_{pH} - I_0)/(I_X - I_0) \quad (4)$$

where I_0 is the initial fluorescence before the heating and I_{pH} and I_X are the corrected intensity at different pHs before and after the addition of Triton X-100, respectively.

3. RESULTS AND DISCUSSION

3.1. Temperature Effect on the Coating Ability. Using the liposome of DPPC/DPPG at 60:40 molar ratio and W2K3 as a model system, we first evaluated the coating ability of peptides on the liposomes. The $M_{w,app}$ of naked liposomes (without coating) was 1.13×10^8 g/mol, corresponding to 1.53×10^5 lipid molecules. The surface area occupied by each lipid was thus about 0.55 nm^2 , close to the values ($0.4\text{--}0.5 \text{ nm}^2$) reported in the literature.^{36–38} The lipid membranes display at least two phases, i.e., “gel phase” and “liquid crystalline phase”. A so-called gel-to-liquid crystalline phase transition occurs at the transition temperature T_c (also referred to as melting temperature). DPPG and DPPC have the same T_c (~ 41 °C) and are highly miscible.^{39,40} However, the redistribution of negatively charged DPPG can occur during the coating of DPPC/DPPG liposome with positively charged peptides. Therefore, the mobility of lipid in the bilayer will inevitably affect the coating efficacy. To test this hypothesis, we studied the temperature effect on the coating ability of W2K3.

Figure 1A shows the stability of uncoated DPPC/DPPG liposomes (60:40 m/m ratio) in HB buffer at 25 °C. At 50 and 250 h, the sample was heated to 50 °C for 30 min and then cooled back to 25 °C. The hydrodynamic radius $R_{h,app}$ (the subscript “app” denotes apparent value) and the radius of gyration $R_{g,app}$ at 50 °C were 10–15 nm larger than those at 25 °C. The swelling of the liposomes at high temperature was caused by the gel to liquid crystalline phase transition.⁴¹ The particle sizes and the molecular weight were unchanged when the temperature was recovered to 25 °C. Clearly, the heat treatment shows no effect on the morphology or the stabilities of the uncoated liposomes.

The situation was quite different in the presence of W2K3. As shown in Figure 1B, the $R_{h,app}$ of the DPPC/DPPG liposomes (60:40 m/m ratio) increased from 65 to ~ 110 nm in 0.5 h after mixed with W2K3 ($\rho_{p/l} = 20$). The size reached ~ 140 nm in 6 h. The excess scattered intensity also increased, indicating the occurrence of aggregation. However, as soon as the samples was heated to 50 °C, the particle size sharply dropped to 80 nm (as indicated by the first arrow in the inset at about 7 h), which was only slightly larger than the size of the uncoated liposomes at 50 °C (76 nm), suggesting the dissociation of the aggregates. When the sample was cooled

back to 25 °C at ~ 8 h, the size was maintained. Both $R_{h,app}$ and $R_{g,app}$ were 80 nm. The ratio of $R_{g,app}/R_{h,app}$ can be used to determine the conformation of a particle. It is well established that the ratio is 0.775 for a solid sphere, 1.0 for a vesicle, and >1.5 for a random coil.⁴² The $R_{g,app}/R_{h,app}$ value of the coated liposomes after heat treatment was close to 1, indicating that the vesicular structure was maintained. The vesicle structure was also confirmed by TEM images. As shown in Figure 2, large unilamellar vesicles with the diameter about 160 nm were clearly seen.

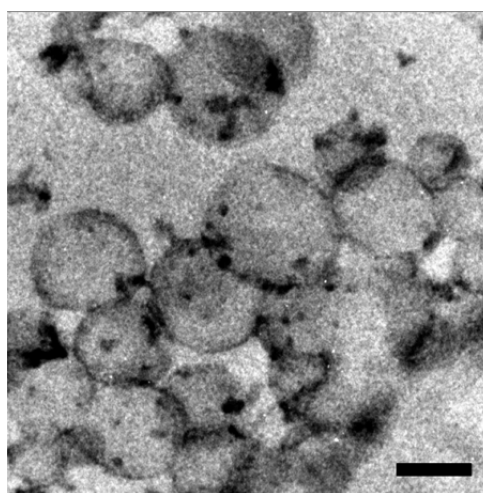


Figure 2. Electronic micrographs of W2K3-coated liposomes. The samples were stained with 1% phosphotungstic acid. $\rho_{p/l} = 20$. Scale bar: 100 nm.

Only one mode was observed during the heating or cooling process (Figure S2). The size distribution of the aggregates formed at 6 h was broader than that of the uncoated or coated liposomes. Interestingly, reheating of the liposome to 50 °C at ~ 9 h, as indicated by the second arrow in the inset, did not generate any effect on the size of the coated liposome, which was different from the behavior of naked liposome (Figure 1A). This suggested that the coating of peptide on the surface prevented the liposomes from swelling at temperatures above T_c when the coating amount was large enough. Figure 1B also shows that the liposome was stable during the following 400 h. Clearly, the treatment by heat enhanced the coating of peptide on the liposome probably by facilitating the close contact of peptides with preferred lipid molecules, since the lipid was mobile at temperatures above T_c . Therefore, heating at 50 °C

for 30 min was conducted 0.5 h after mixing in the following experiments.

The coated peptide over liposome ratio is a key parameter to evaluate the coating ability. Three W2K3/liposome samples with the mixing $\rho_{p/l}$ ratios being 20, 1.0, and 0.60 were prepared. The number of the coated peptides was determined by the molecular weight (M_w) difference of the liposome before and after coating. The charge ratio was calculated accordingly. As shown in Figure 3, the coated W2K3/liposome charge ratio

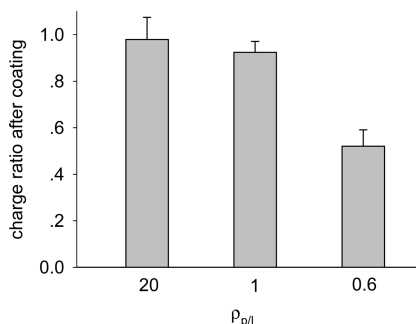


Figure 3. Charge ratio of coated W2K3 to DPPC/DPPG liposomes (60:40 m/m ratio) at different mixing $\rho_{p/l}$ values.

was only 0.98 at $\rho_{p/l} = 20$, suggesting that most of the peptides stayed as free molecules in the solution. While at $\rho_{p/l}$ being 1.0 and 0.60, the coated ratios were 0.92 and 0.52, respectively. Most of (about 90%) the peptides were coated on the liposome. This also indicated that the electrostatic attraction was the major driving force for the coating of W2K3 on DPPC/DPPG liposomes (60:40 m/m ratio). Moreover, the aggregation of liposome at $\rho_{p/l}$ ratios lower than 1 was not prominent before the heat treatment at 50 °C (Figure S2), implying that the peptide was not only able to coat the liposome but also induced interparticle aggregation if the amount was excess.

3.2. Difference between K and R. Arginine-rich peptides have been reported to be able to translocate through cell membranes. They are potential carriers of DNA and proteins.^{43–45} The coating of the liposome by W2R3 was also facilitated by heat treatment, similar to the coating by W2K3. Figure 4 compares the coating ability of W2R3 and W2K3 on two different liposome surfaces at 1 h after heat treatment. W2G3 was used as a control. To ensure enough peptides were available, $\rho_{p/l}$ of 20 was chosen. The coating of

peptides was stronger on the liposome with higher content of charged lipids. Compared with those of W2K3 or W2R3, the coating of W2G3, which contains no charged residues, was negligible. Both results suggested that the electrostatic attraction was a major driving force for coating. However, the coating amount of W2R3 was always larger than that of W2K3, even though they contained the same positive charges. The difference was even larger on the liposome surface with higher charge density (Figure 4B). This indicated that the parameters other than electrostatic interactions also played a role during the coating.

Figure 5 shows the zeta potential of the liposomes of varying DPPG content before and after the coating with peptides. The

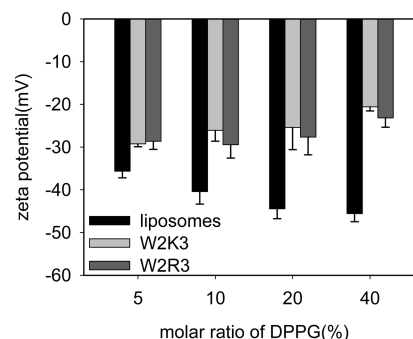


Figure 5. Zeta potential of DPPC/DPPG liposomes with and without coated peptides in HB buffer. $\rho_{p/l} = 20$. Temperature: 25 °C.

zeta potential of the negatively charged liposomes changed from -34 to -48 mV as the DPPG content increased from 5 to 40%. The coating of the peptide resulted in a decrease of the negative zeta potentials. The degree of decrease was heavier as the DPPG content increased. This confirmed that the major driving force for coating was electrostatic attraction, in agreement with the LLS result. Each W2K3 or W2R3 contains three charges. In most of the cases, the number of positive charges attached on the liposome surface, on the basis of the data shown in Figure 4, was more than the number of negative charges from DPPG, especially in the case of W2R3. However, no charge reversal was observed in all the cases. We attributed it to the location of the positive charges in peptides. In W2K3 or W2R3, the charged amino acids were located near the C-terminal of the peptides. They were tightly bound to the membrane surface, leaving the neutral segments $-GGNNN$ facing outward. Similar to the behavior of poly(ethylene

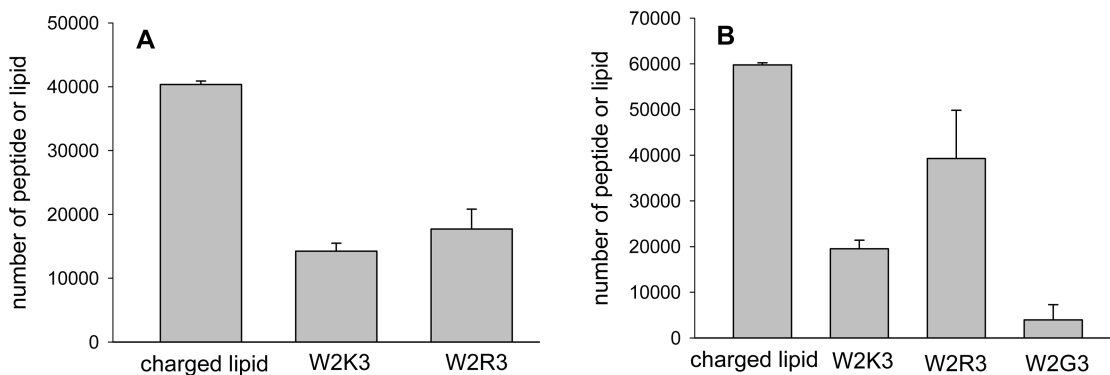


Figure 4. Number of coated peptides on (A) DPPC/DPPG liposomes (80:20 m/m ratio) and (B) DPPC/DPPG liposomes (60:40 m/m ratio) in HB buffer. The first bar in panels A and B represents the number of charged lipids in each liposome. $\rho_{p/l} = 20$. Temperature = 25 °C.

glycol),^{46,47} this neural layer effectively screened the surface charges introduced by the charged peptides, preventing the occurrence of charge reversal.

The binding of peptide should involve the tryptophan residues since they can strongly attach to the interfacial region of lipid bilayers.^{26–28} Figure S3 shows the fluorescence emission spectra of W2K3 and W2R3 in HB buffer with or without liposomes. To eliminate the influence of free peptides, the mixture with $\rho_{p/l} = 1.0$ was chosen. The fluorescence was derived mainly from the Trp residue. Its maximum emission wavelength (λ_{\max}) at different situations is listed in Table 1.

Table 1. Maximal Trp Emission Wavelength (λ_{\max}) with and without Liposomes^a

lipid ratio of DPPC/DPPG (% m/m)	W2R3	W2K3
	λ_{\max} (nm)	λ_{\max} (nm)
100:0	355	356
95:5	354	356
80:20	348	352
60:40	347	351

^a $\lambda_{\text{ex}} = 280$ nm, HB buffer.

Without liposomes, the λ_{\max} was 355 ± 1 nm in HB buffer, and it was independent of the peptide sequence. The λ_{\max} was shift to lower wavelength with the addition of DPPC/DPPG liposomes. The shift was stronger with increasing content of DPPG in the liposome. As shown in Table 1, the λ_{\max} value was barely changed in the presence of liposome with 5% DPPG, but it decreased by 6–8 nm for W2R3 when the content of DPPG increased to 40%. As for W2K3, a blue-shift of 5 nm was measured when incubated with liposomes of the same charge density. The level of wavelength shift was similar to the values reported in the literature.⁴⁸ The blue-shift was attributed to the interaction of indole with the polar solvent. Following excitation, the energy of the excited state was related to the solvent polarity.⁴⁹ The increase of the solvent polarity resulted in emission at lower energies or longer wavelengths.⁵⁰ Conversely, a blue-shift occurred when the solvent polarity decreased, indicating that the environment of Trp residues became more hydrophobic. In other words, the Trp residues reached the interface region of the bilayer. Clearly, the binding of Trp residues in the bilayer was facilitated by the electrostatic interactions because no blue-shift was observed in the same situation for W2G3.

3.3. Salt Effect. The strength and working range of the electrostatic interaction are sensitive to ionic strength. The coating ability of peptides on the liposome in the physiological salt concentration was measured by LLS. Figure S4 shows the coating amount of W2R3 and W2K3 on DPPC/DPPG liposome (80:20 m/m) in HBS buffer. Similar to the results in HB, both W2R3 and W2K3 can coat the liposome surface, and the coating ability of W2R3 was stronger. The major difference was that the amount of coated peptide, for both W2R3 and W2K3, decreased in HBS buffers. Stradner et al.⁵¹ have reported the coexistence of long-ranged electrostatic repulsion and short-ranged electrostatic attraction among charged colloidal particles. In the mixture of peptide and liposome, the long-ranged electrostatic repulsion was referred to the interactions among peptides, while the short-ranged electrostatic attraction was referred to the interactions between DPPG and peptides. The addition of NaCl screened both electrostatic interactions. But the effect on the short-ranged electrostatic attraction was stronger than that on the repulsion in the studied salt concentration, leading to a weakening of the peptide coating on the liposome.

3.4. pH Sensitivity of Liposomes Coated with Peptides. The basic amino acids can be protonated or deprotonated in response to the change in pH.⁵² Therefore, the coating of W2R3 and W2K3 should be able to render the liposome pH- responsive properties. The naked DPPC/DPPG liposome (60:40 m/m ratio) was stable in HBS buffer at pH values ranging from 5.5 to 7.4. Both the scattered intensity (Figure S5) and the size distribution (Figure S6) were constant in 200 h at 37 °C. However, the behavior of the liposome was changed when coated with peptides, and the change was also peptide dependent.

At mixing ratio $\rho_{p/l} = 1.0$, most W2R3 or W2K3 molecules coated on the surface of DPPC/DPPG liposome (60:40 m/m ratio). The free peptides in solution were negligible. For the liposome coated with W2K3, its size distribution was close to that of the naked liposome, and no prominent changes in either size (Figure S7) or scattered intensity (Figure 6A) was observed in the studied time period at pH 7.4, suggesting that the coated liposomes were stable in solution of neutral pH. However, the scattered intensity sharply decreased and reached the platform in ~ 80 h at pH 5.5 (Figure 6A). The size remained almost constant, but the size distribution broadened in the studied time period as shown in Figure 7.

For the liposome coated with W2R3, its size distribution was broader than that of the naked liposome right after coating at

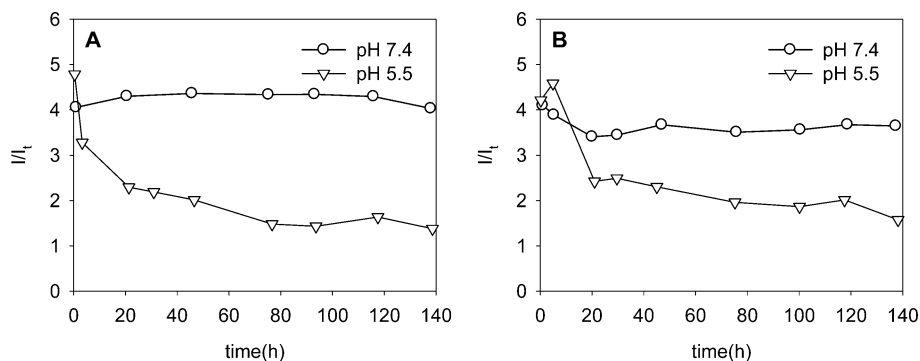


Figure 6. Time dependence of the intensity of DPPC/DPPG liposomes (60:40 m/m ratio) coated with (A) W2K3 and (B) W2R3 at different pHs in HBS. $\rho_{p/l} = 1.0$. Temperature = 37 °C.

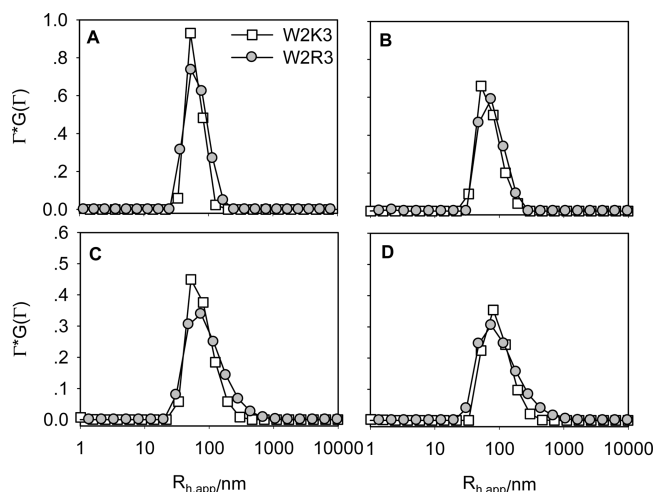


Figure 7. Size distribution of DPPC/DPPG liposomes (60:40 m/m ratio) coated with W2K3 or W2R3 at (A) 1, (B) 20, (C) 75, and (D) 120 h at pH 5.5. Scattering angle: 30° . $\rho_{p/l} = 1.0$. Temperature = 37°C .

pH 7.4. But no further changes in size distribution were observed during the studied time period at neutral pH (Figure S7). Moreover, the excess scattered intensity decreased in the first 20 h and then kept almost constant thereafter. Since this phenomenon was not observed in the case of W2K3, we attributed to the effect of arginine residues, which were able to deform the vesicle structures after binding to the liposome surface. At pH 5.5, the scattered intensity exhibited a similar behavior as that in the case of W2K3 (Figure 6B). However, the particle size became slightly larger and the size distribution became broader with time. The decrease in the scattered intensity together with the gradual increase of the particle size suggested the rupture of liposomes at pH 5.5 in the presence of both W2K3 and W2R3. TEM images (Figure S8), which showed rupture and deformation of the liposome, confirmed LLS results.

The rupture of the liposome and even phase separation were more obvious at mixing ratio $\rho_{p/l} = 20$ (Figures S9 and S10). The disturbance of the membrane by W2R3 was different from that by W2K3. Although both were positively charged in their physiological state, there was increasing evidence that they differed in the interaction with lipid membranes. It was already known that polyarginine can cause leakage of neutral or anionic vesicles.⁵² It was already reported that the delocalized charge of the guanidinium group of arginine was able to mediate the translocation of arginine-rich oligo/polymers across bulk and lipid bilayer membranes.^{53,54} The multivalent nature of the guanidinium group allowed Arg to simultaneously interact with both phosphate and glycerol groups and thus changed the phase behavior of peptide–lipid mixtures.⁵⁵

3.5. Controlled Release of Calcein from Coated Liposome. Liposomes have been widely studied as drug carriers. The physical coating of peptide rendered the liposome some attractive features, such as the pH-responsive behavior. Using calcein as the model drug and fluorescence label, we examined the release of calcein from the coated liposome at different pHs. The concentration of calcein encapsulated in liposomes was 80 mM, at which concentration its fluorescence was self-quenched.⁵⁶ The leakage of calcein from the liposome resulted in an increase of fluorescence, which can be used to determine the concentration. It was known that the leakage of

the liposome was the fastest around T_c . A heating and cooling cycle at fixed rate was employed to induce the release of the cargo from liposomes. For the naked liposome, the percentage (F) of the released calcein was 4.4% at pH 7.4 and 16.5% at pH 5.5 (Figure 8), indicating that the permeability of uncoated liposomes was negligible at neutral pH but a little strengthened at acid environment.

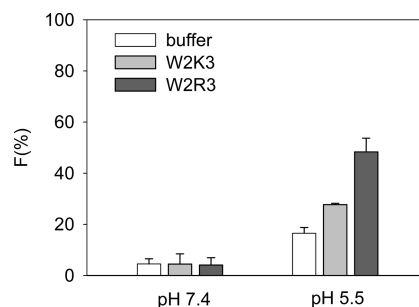


Figure 8. Percentage (F) of the calcein released from naked liposomes (white bar) and the liposomes coated with W2K3 (gray bar) or W2R3 (black bar) at pH 7.4 and pH 5.5. $\rho_{p/l} = 1$.

For the liposome coated with W2K3 or W2R3 at $\rho_{p/l} = 1.0$, the percentage of calcein released at pH 7.4 was the same as that of uncoated liposome (Figure 8). However, at pH = 5.5, the release percentage increased to 27.7% for W2K3 and 48.3% for W2R3. This further confirmed that W2R3 possessed stronger ability than W2K3 in disrupting lipid membrane at acidic pH.

Figure 9 shows the calcein fluorescence curve of the liposomes coated with W2K3 during the heating and cooling cycle. It was clear that, at both pHs, the dramatic change in fluorescence intensity largely occurred at $41\text{--}42^\circ\text{C}$, around the T_c of the liposome. Uncoated liposomes (Figure S11) showed the same tendency. This suggested that the coated peptide did not change the phase transition temperature of the liposomes. In the case of the liposomes coated with W2R3 (Figure S12), besides the region of phase transition temperature, continued leakage was also observed at temperatures above that.

The heavy release of the calcein from the coated liposome could be explained by the defects at the domain boundaries within the membranes.^{57,58} Upon the adsorption of cationic peptides onto a membrane consisting of negatively charged and neutral lipids, the strong electrostatic interaction may induce changes in lipid composition at the binding site on the premise of the lateral fluidity of membranes.⁵⁹ The changes in membrane fluidity at T_c afforded the ability of negatively charged lipids to migrate and adjust their concentration at the binding site and hence strengthened the electrostatic interaction between the peptides and the lipid membrane. The formation of the domains in rich of charged lipid and peptide resulted in microphase separation on the membrane surface. This was confirmed on giant unilamellar vesicles in the presence of W2K3 or W2R3 (Figure S13). The interface between the domains was delicate and contained defects. The release of the cargo was thus significantly enhanced. For W2R3-coated liposomes, the deep penetration of peptides inside the membrane, as demonstrated by the larger blue-shift in Table 1, generated heavier leakage, even at temperatures higher than T_c .

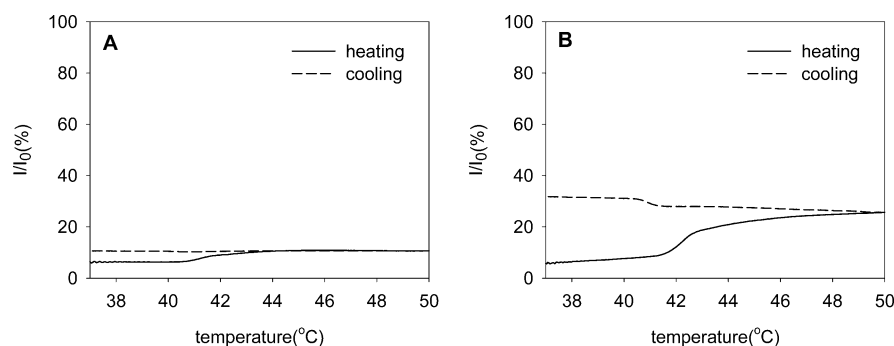


Figure 9. Temperature dependence of the fluorescence from W2K3-coated DPPC/DPPG liposomes (60:40 m/m ratio) encapsulated with calcein at (A) pH 7.4 and (B) pH 5.5. $\rho_{p/1} = 1$. Heating rate: 0.1 °C/min. Cooling rate: 0.2 °C/min. $\lambda_{\text{ex}} = 490$ nm and $\lambda_{\text{em}} = 520$ nm.

4. CONCLUSIONS

We demonstrated the creation of peptide-coated liposomes by using charged peptides containing Trp residues. The binding of water-soluble peptides to lipid membranes was mainly mediated by the electrostatic interaction between the peptides' cationic side groups and the acidic lipids as well as the "anchoring" of Trp residuals in the interfacial region of lipid bilayers. The amount of the coated peptides was larger for W2R3 than that for W2K3, while liposomes coated with W2K3 showed better stability at both neutral and acidic environment. The coating efficiency of the peptide and the permeability of coated liposome were governed by the phase behavior, i.e., the temperature. The generated peptide layer could allow both pH- and temperature-induced release of the encapsulated cargos.

The liposome externally coated with peptide, abbreviated as pepsome, mimics the protein delivery vehicle inside cells.⁶⁰ It combined the vesicle structure of liposome and the functions of peptide, yielding many attractive features, such as easy cargo loading, controlled release, and specific targeting. Moreover, the biocompatibility and biodegradability of lipid and peptide rendered pepsome a promising vehicle to deliver drugs and genes in a safe and efficient manner.

■ ASSOCIATED CONTENT

Supporting Information

Size distribution and stability of DPPC/DPPG liposomes at varying conditions; the fluorescence emission spectra of peptides; TEM images of coated liposomes at pH 5.5; the temperature dependence of the fluorescence from uncoated and W2R3 coated liposomes encapsulated with calcein; giant unilamellar vesicles with peptides. This material is available free of charge via the Internet at <http://pubs.acs.org>.

■ AUTHOR INFORMATION

Corresponding Author

*Tel +86-10-62756170, Fax 86-10-62751708, e-mail dliang@pku.edu.cn (D.L.).

Notes

The authors declare no competing financial interest.

■ ACKNOWLEDGMENTS

Financial support of this work from the National Natural Science Foundation of China (21074005), the National Basic Research Program of China (973 Program, 2012CB821500), and the Ministry of Education in China is gratefully acknowledged.

■ REFERENCES

- (1) Cattel, L.; Ceruti, M.; Dosio, F. From conventional to stealth liposomes: a new frontier in cancer chemotherapy. *J. Chemother.* **2004**, *16*, 94–97.
- (2) Schroeder, A.; Levins, C. G.; Cortez, C.; Langer, R.; Anderson, D. G. Lipid-based nanotherapeutics for siRNA delivery. *J. Int. Med.* **2010**, *267*, 9–21.
- (3) Liu, M.; Gan, L.; Chen, L.; Xu, Z.; Zhu, D.; Hao, Z.; Chen, L. Supramolecular core-shell nanosilica@liposome nanocapsules for drug delivery. *Langmuir* **2012**, *28*, 10725–10732.
- (4) Sanko, N.; Alund, S. J.; Hiorth, M.; Kjoniksen, A.-L.; Smistad, G. Studies on pectin coating of liposomes for drug delivery. *Colloids Surf., B* **2011**, *88*, 664–673.
- (5) Fujimoto, K.; Toyoda, T.; Fukui, Y. Preparation of bionanocapsules by the layer-by-layer deposition of polypeptides onto a liposome. *Macromolecules* **2007**, *40*, 5122–5128.
- (6) Fukui, Y.; Fujimoto, K. The preparation of sugar polymer-coated nanocapsules by the layer-by-layer deposition on the liposome. *Langmuir* **2009**, *25*, 10020–10025.
- (7) Barea, M. J.; Jenkins, M. J.; Gaber, M. H.; Bridson, R. H. Evaluation of liposomes coated with a pH responsive polymer. *Int. J. Pharm.* **2010**, *402*, 89–94.
- (8) Fukui, Y.; Fujimoto, K. Control in mineralization by the polysaccharide-coated liposome via the counter-diffusion of ions. *Chem. Mater.* **2011**, *23*, 4701–4708.
- (9) Yamamoto, S.; Fukui, Y.; Kaihara, S.; Fujimoto, K. Preparation and assembly of poly(arginine)-coated liposomes to create a free-standing bioscaffold. *Langmuir* **2011**, *27*, 9576–9582.
- (10) Garg, A.; Kokkoli, E. pH-sensitive PEGylated liposomes functionalized with a fibronectin-mimetic peptide show enhanced intracellular delivery to colon cancer cells. *Curr. Pharm. Biotechnol.* **2011**, *12*, 1135–1143.
- (11) Drummond, D. C.; Zignani, M.; Leroux, J. C. Current status of pH-sensitive liposomes in drug delivery. *Prog. Lipid Res.* **2000**, *39*, 409–460.
- (12) Rofstad, E. K.; Mathiesen, B.; Kindem, K.; Galappathi, K. Acidic extracellular pH promotes experimental metastasis of human melanoma cells in athymic nude mice. *Cancer Res.* **2006**, *66*, 6699–6707.
- (13) Schmaljohann, D. Thermo- and pH-responsive polymers in drug delivery. *Adv. Drug Delivery Rev.* **2006**, *58*, 1655–1670.
- (14) Vaupel, P.; Kallinowski, F.; Okunieff, P. Blood flow, oxygen and nutrient supply, and metabolic microenvironment of human tumors: a review. *Cancer Res.* **1989**, *49*, 6449–6465.
- (15) Grabe, M.; Oster, G. Regulation of organelle acidity. *J. Gen. Physiol.* **2001**, *117*, 329–343.
- (16) Petschnigg, J.; Moe, O. W.; Staglar, I. Using yeast as a model to study membrane proteins. *Curr. Opin. Nephrol. Hypertens.* **2011**, *20*, 425–432.
- (17) Levine, R. M.; Scott, C. M.; Kokkoli, E. Peptide functionalized nanoparticles for nonviral gene delivery. *Soft Matter* **2013**, *9*, 985–1004.

- (18) Tooze, S. A. Biogenesis of secretory granules in the trans-Golgi network of neuroendocrine and endocrine cells. *Biochim. Biophys. Acta, Mol. Cell Res.* **1998**, *1404*, 231–244.
- (19) Prado, V. F.; Prado, M. A. M. Signals involved in targeting membrane proteins to synaptic vesicles. *Cell Mol. Neurobiol.* **2002**, *22*, 565–577.
- (20) Pearce, T. R.; Shroff, K.; Kokkoli, E. Peptide targeted lipid nanoparticles for anticancer drug delivery. *Adv. Mater.* **2012**, *24*, 3803–3822.
- (21) Nakase, I.; Akita, H.; Kogure, K.; Gräslund, A.; Langel, Ü.; Harashima, H.; Futaki, S. Efficient intracellular delivery of nucleic acid pharmaceuticals using cell-penetrating peptides. *Acc. Chem. Res.* **2012**, *45*, 1132–1139.
- (22) Khalil, I. A.; Kogure, K.; Futaki, S.; Hama, S.; Akita, H.; Ueno, M.; Kishida, H.; Kudoh, M.; Mishina, Y.; Kataoka, K.; Yamada, M.; Harashima, H. Octaarginine-modified multifunctional envelope-type nanoparticles for gene delivery. *Gene Ther.* **2007**, *14*, 682–689.
- (23) Li, W. J.; Nicol, F.; Szoka, F. C. GALA: a designed synthetic pH-responsive amphipathic peptide with applications in drug and gene delivery. *Adv. Drug Delivery Rev.* **2004**, *56*, 967–985.
- (24) Kakudo, T.; Chaki, S.; Futaki, S.; Nakase, I.; Akaji, K.; Kawakami, T.; Maruyama, K.; Kamiya, H.; Harashima, H. Transferrin-modified liposomes equipped with a pH-sensitive fusogenic peptide: An artificial viral-like delivery system. *Biochemistry* **2004**, *43*, 5618–5628.
- (25) Wimley, W. C.; White, S. H. Experimentally determined hydrophobicity scale for proteins at membrane interfaces. *Nat. Struct. Biol.* **1996**, *3*, 842–848.
- (26) de Planque, M. R. R.; Bonev, B. B.; Demmers, J. A. A.; Greathouse, D. V.; Koeppe, R. E.; Separovic, F.; Watts, A.; Killian, J. A. Interfacial anchor properties of tryptophan residues in transmembrane peptides can dominate over hydrophobic matching effects in peptide-lipid interactions. *Biochemistry* **2003**, *42*, 5341–5348.
- (27) van der Wel, P. C. A.; Reed, N. D.; Greathouse, D. V.; Koeppe, R. E., II Orientation and motion of tryptophan interfacial anchors in membrane-spanning peptides. *Biochemistry* **2007**, *46*, 7514–7524.
- (28) Norman, K. E.; Nymeyer, H. Indole localization in lipid membranes revealed by molecular simulation. *Biophys. J.* **2006**, *91*, 2046–2054.
- (29) Blaser, G.; Sanderson, J. M.; Wilson, M. R. Free-energy relationships for the interactions of tryptophan with phosphocholines. *Org. Biomol. Chem.* **2009**, *7*, 5119–5128.
- (30) Christiaens, B.; Symoens, S.; Verheyden, S.; Engelborghs, Y.; Joliot, A.; Prochiantz, A.; Vandekerckhove, J.; Rosseneu, M.; Vanloo, B. Tryptophan fluorescence study of the interaction of penetratin peptides with model membranes. *Eur. J. Biochem.* **2002**, *269*, 5101–5101.
- (31) Clark, E. H.; East, J. M.; Lee, A. G. The role of tryptophan residues in an integral membrane protein: diacylglycerol kinase. *Biochemistry* **2003**, *42*, 11065–11073.
- (32) Okuda, T.; Sugiyama, A.; Niidome, T.; Aoyagi, H. Characters of dendritic poly(L-lysine) analogues with the terminal lysines replaced with arginines and histidines as gene carriers in vitro. *Biomaterials* **2004**, *25*, 537–544.
- (33) Findlay, E. J.; Barton, P. G. Phase behavior of synthetic phosphatidylglycerols and binary-mixtures with phosphatidylcholines in presence and absence of calcium-ions. *Biochemistry* **1978**, *17*, 2400–2405.
- (34) Bartlett, G. R. Phosphorus assay in column chromatography. *J. Biol. Chem.* **1959**, *234*, 466–468.
- (35) Vacklin, H. P.; Tiberg, F.; Fragneto, G.; Thomas, R. K. Phospholipase A(2) hydrolysis of supported phospholipid bilayers: A neutron reflectivity and ellipsometry study. *Biochemistry* **2005**, *44*, 2811–2821.
- (36) Tristramnagle, S.; Zhang, R.; Suter, R. M.; Worthington, C. R.; Sun, W. J.; Nagle, J. F. Measurement of chain tilt angle in fully hydrated bilayers of gel phase lecithins. *Biophys. J.* **1993**, *64*, 1097–1109.
- (37) Pabst, G.; Danner, S.; Karmakar, S.; Deutsch, G.; Raghunathan, V. A. On the propensity of phosphatidylglycerols to form interdigitated phases. *Biophys. J.* **2007**, *93*, 513–525.
- (38) Nagle, J. F.; Tristram-Nagle, S. Structure of lipid bilayers. *Biochim. Biophys. Acta, Rev. Biomembr.* **2000**, *1469*, 159–195.
- (39) Nibu, Y.; Inoue, T.; Motoda, I. Effect of headgroup type on the miscibility of homologous phospholipids with different acyl-chain lengths in hydrated bilayer. *Biophys. Chem.* **1995**, *56*, 273–280.
- (40) Mansour, H.; Wang, D. S.; Chen, C. S.; Zograf, G. Comparison of bilayer and monolayer properties of phospholipid systems containing dipalmitoylphosphatidylglycerol and dipalmitoylphosphatidylinositol. *Langmuir* **2001**, *17*, 6622–6632.
- (41) Taylor, K. M. G.; Morris, R. M. Thermal-analysis of phase-transition behavior in liposomes. *Thermochim. Acta* **1995**, *248*, 289–301.
- (42) Burchard, W. Static and dynamic light-scattering from branched polymers and bio-polymers. *Adv. Polym. Sci.* **1983**, *48*, 1–124.
- (43) Futaki, S.; Suzuki, T.; Ohashi, W.; Yagami, T.; Tanaka, S.; Ueda, K.; Sugiura, Y. Arginine-rich peptides - An abundant source of membrane-permeable peptides having potential as carriers for intracellular protein delivery. *J. Biol. Chem.* **2001**, *276*, 5836–5840.
- (44) Futaki, S.; Ohashi, W.; Suzuki, T.; Niwa, M.; Tanaka, S.; Ueda, K.; Harashima, H.; Sugiura, Y. Stearilated arginine-rich peptides: A new class of transfection systems. *Bioconjugate Chem.* **2001**, *12*, 1005–1011.
- (45) Schmidt, N.; Mishra, A.; Lai, G. H.; Wong, G. C. L. Arginine-rich cell-penetrating peptides. *FEBS Lett.* **2010**, *584*, 1806–1813.
- (46) Levchenko, T. S.; Rammohan, R.; Lukyanov, A. N.; Whiteman, K. R.; Torchilin, V. P. Liposome clearance in mice: the effect of a separate and combined presence of surface charge and polymer coating. *Int. J. Pharm.* **2002**, *240*, 95–102.
- (47) Phillips, N. C.; Heydari, C.; Saoud, M. Reduction of cationic liposome zeta (zeta) potential by amphiphilic poly(ethylene glycol) derivatives. *Eur. J. Pharm. Sci.* **1996**, *4*, S43–S43.
- (48) Chen, Y.; Barkley, M. D. Toward understanding tryptophan fluorescence in proteins. *Biochemistry* **1998**, *37*, 9976–9982.
- (49) Strickla, Eh; Billups, C.; Kay, E. Effects of hydrogen-bonding and solvents upon tryptophanyl 1-l-a absorption-band - studies using 2,3-dimethylindole. *Biochemistry* **1972**, *11*, 3657–8.
- (50) *Principles of Fluorescence Spectroscopy*; Lakowicz, J. R., Ed.; Kluwer Academic/Plenum Publishers: New York, 1999; pp 185–186.
- (51) Stradner, A.; Sedgwick, H.; Cardinaux, F.; Poon, W. C. K.; Egelhaaf, S. U.; Schurtenberger, P. Equilibrium cluster formation in concentrated protein solutions and colloids. *Nature* **2004**, *432*, 492–495.
- (52) Bondeson, J.; Sundler, R. Promotion of acid-induced membrane fusion by basic peptides. Amino acid and phospholipid specificities. *Biochim. Biophys. Acta, Biomembr.* **1990**, *1026*, 186–194.
- (53) Sakai, N.; Matile, S. Anion-mediated transfer of polyarginine across liquid and bilayer membranes. *J. Am. Chem. Soc.* **2003**, *125*, 14348–14356.
- (54) Stromstedt, A. A.; Ringstad, L.; Schmidtchen, A.; Malmsten, M. Interaction between amphiphilic peptides and phospholipid membranes. *Curr. Opin. Colloid Interface Sci.* **2010**, *15*, 467–478.
- (55) Wu, Z.; Cui, Q.; Yethiraj, A. Why do arginine and lysine organize lipids differently? Insights from coarse-grained and atomistic simulations. *J. Phys. Chem. B* **2013**, *117*, 12145–12156.
- (56) Allen, T. M.; Cleland, L. G. Serum-induced leakage of liposome contents. *Biochim. Biophys. Acta* **1980**, *597*, 418–426.
- (57) Papahadj, D.; Jacobson, K.; Nir, S.; Isac, T. Phase-transitions in phospholipid vesicles - fluorescence polarization and permeability measurements concerning effect of temperature and cholesterol. *Biochim. Biophys. Acta* **1973**, *311*, 330–348.
- (58) Cruzeirohansson, L.; Ipsen, J. H.; Mouritsen, O. G. Intrinsic molecules in lipid-membranes change the lipid-domain interfacial area - cholesterol at domain interfaces. *Biochim. Biophys. Acta* **1989**, *979*, 166–176.

(59) Mbamala, E. C.; Ben-Shaul, A.; May, S. Domain formation induced by the adsorption of charged proteins on mixed lipid membranes. *Biophys. J.* **2005**, *88*, 1702–1714.

(60) Bonifacino, J. S.; Glick, B. S. The mechanisms of vesicle budding and fusion. *Cell* **2004**, *116*, 153–166.

Supporting Information for

Liposomes Physically Coated with Peptides: Preparation and Characterization

Cuicui Su¹, Yuqiong Xia², Jianbo Sun¹, Nan Wang¹, Lin Zhu¹, Tao Chen³, Yanyi Huang³ and Dehai Liang^{1,}*

¹Beijing National Laboratory for Molecular Sciences and the Key Laboratory of Polymer Chemistry and Physics of Ministry of Education, College of Chemistry and Molecular Engineering, Peking University, Beijing, China, 100871;

²School of Life Sciences and Technology, Xidian University, Xi'an, Shanxi, 710126 China

³Biodynamic Optical Imaging Center (BIOPIC), Peking University, Beijing 100871, China

Corresponding Author * Dehai Liang, Tel: +86-10-62756170, Fax: 86-10-62751708, Email:

dliang@pku.edu.cn

Temperature effect on the coating ability

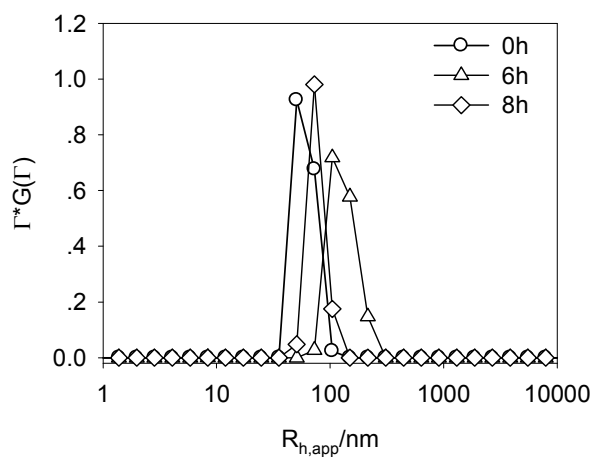


Figure S1. Size distribution of DPPC/DPPG liposomes (60:40 m/m ratio) in HB at different time points after added to W2K3 solutions. Scattering angle: 30°. Temperature = 25 °C. $\rho_{p/l} = 20$.

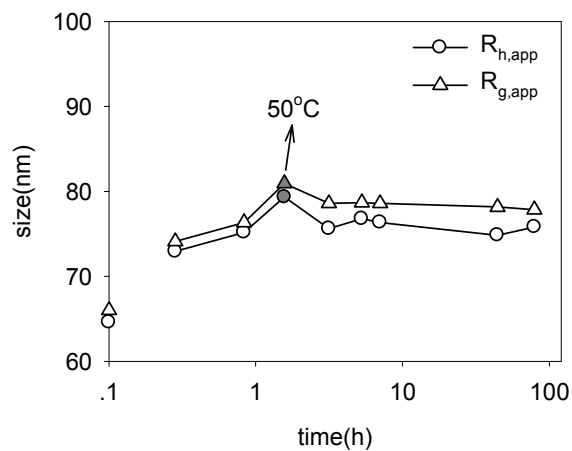


Figure S2. Time dependence of the sizes of DPPC/DPPG liposomes (60:40 m/m ratio) after added into W2K3 ($\rho_{p/l} = 1$) in HB at different time points. Temperature: 25 °C. The filled symbols show the results at 50 °C.

Fluorescence measurements

The fluorescence of Trp was measured at 25 °C in a spectrofluorometer (FLS920, Edinburgh Instruments Ltd.) equipped with a temperature controller. Emission spectra were recorded from 300 nm to 450 nm with an excitation wavelength of 280 nm. The scattered light was corrected by subtracting the corresponding intensity of pure liposomes from the mixture.

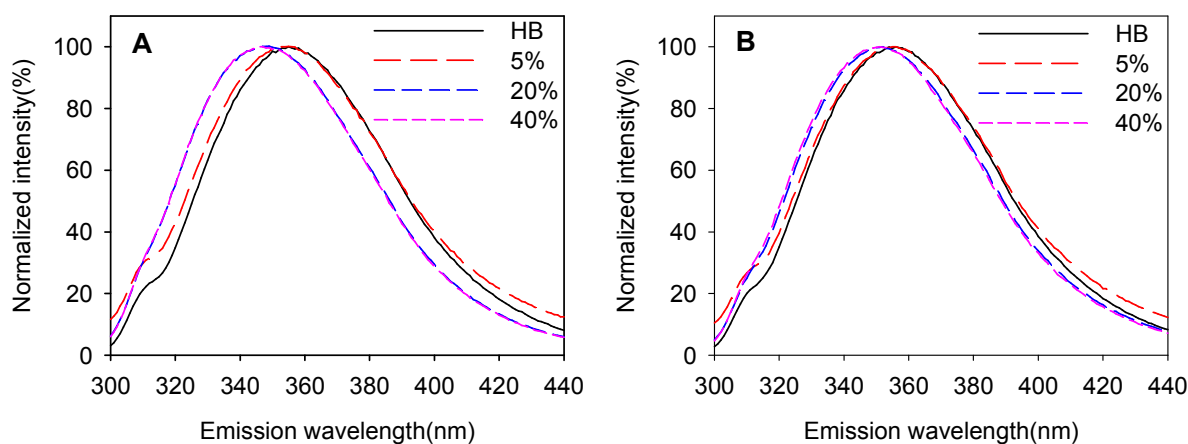


Figure S3. Fluorescence emission spectra of (A) W2R3 and (B) W2K3 in HB buffer before and after mixing with liposomes containing different DPPG content. $\lambda_{\text{ex}} = 280$ nm. Temperature: 25 °C.

Coating amount in HBS

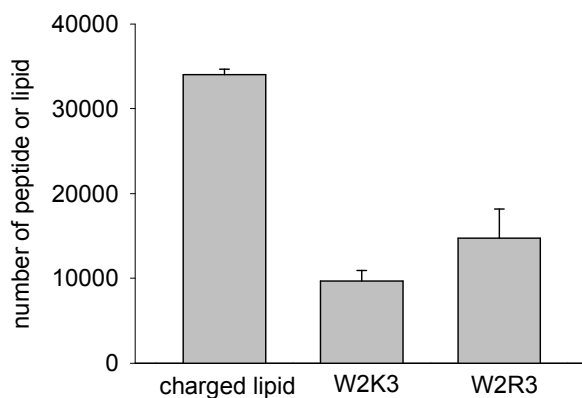


Figure S4. The number of coated peptides when DPPC/DPPG liposomes (80:20 m/m ratio) were added to peptide solutions in HBS buffer. The first bar represents the number of charged lipids in the liposome. $\rho_{p/l} = 20$. Temperature = 25 °C.

Stability at different pHs

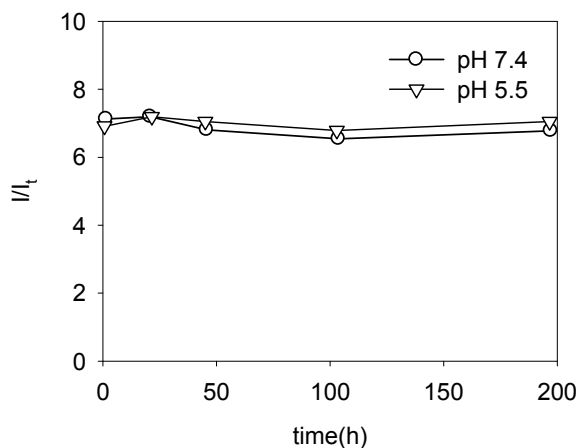


Figure S5. Changes of the intensity of DPPC/DPPG liposomes (60:40 m/m ratio) with time at different pHs in HBS. Temperature = 37 °C.

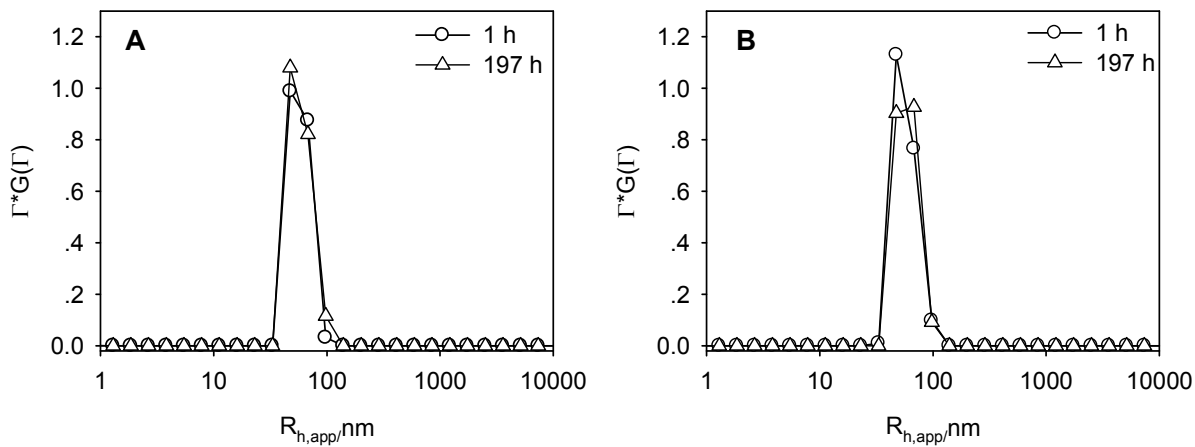


Figure S6. Size distribution of DPPC/DPPG liposomes (60:40 m/m ratio) in HBS at A) pH 7.4 and B) pH 5.5. Scattering angle: 30° . Temperature = 37°C .

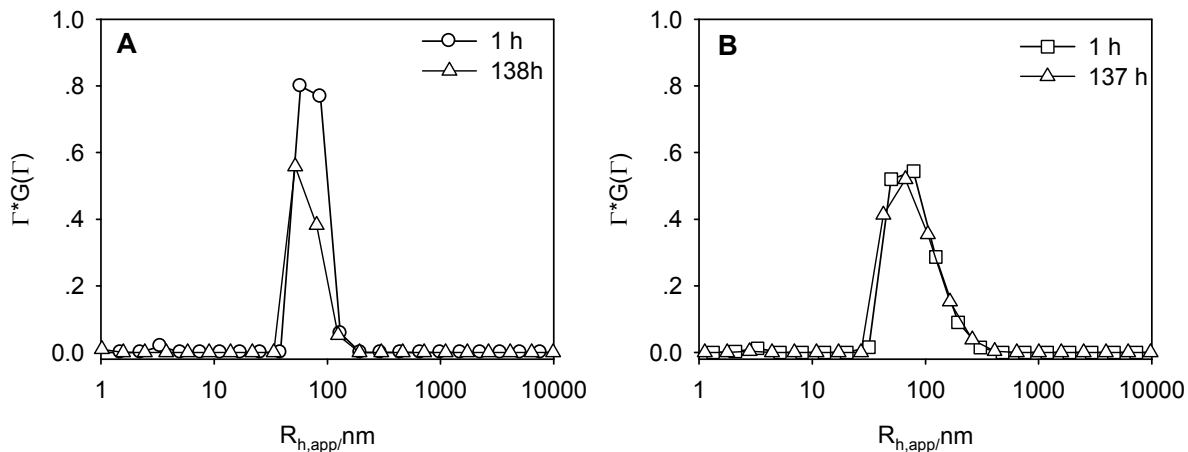


Figure S7. Size distribution of DPPC/DPPG liposomes (60:40 m/m ratio) coated by A) W2K3 and B) W2R3 at different time point at pH 7.4. Scattering angle: 30° . Temperature = 37°C .

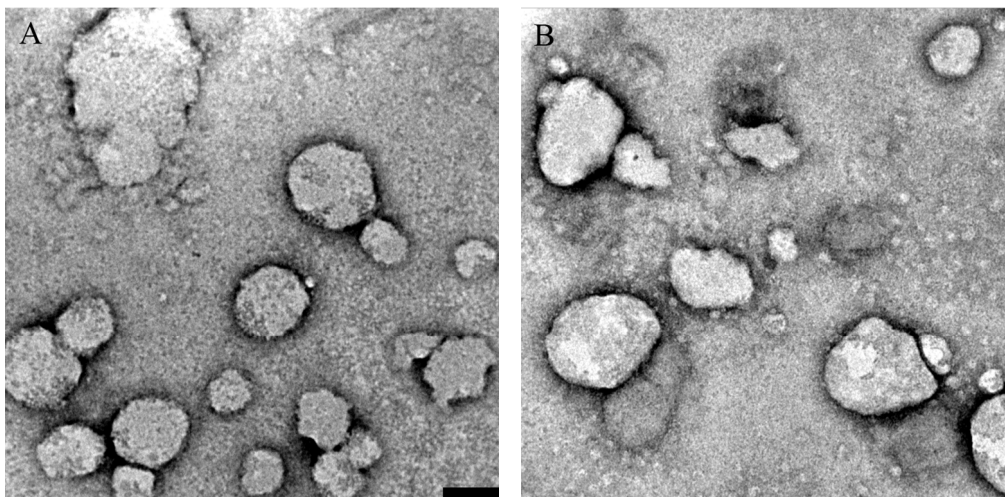


Figure S8. Electronic micrographs of the liposomes coated with A) W2K3 and B) W2R3 for 24 hrs. pH = 5.5. The samples were stained with 1% phosphotungstic acid. $\rho_{p/l} = 1$. Scale bar: 100 nm.

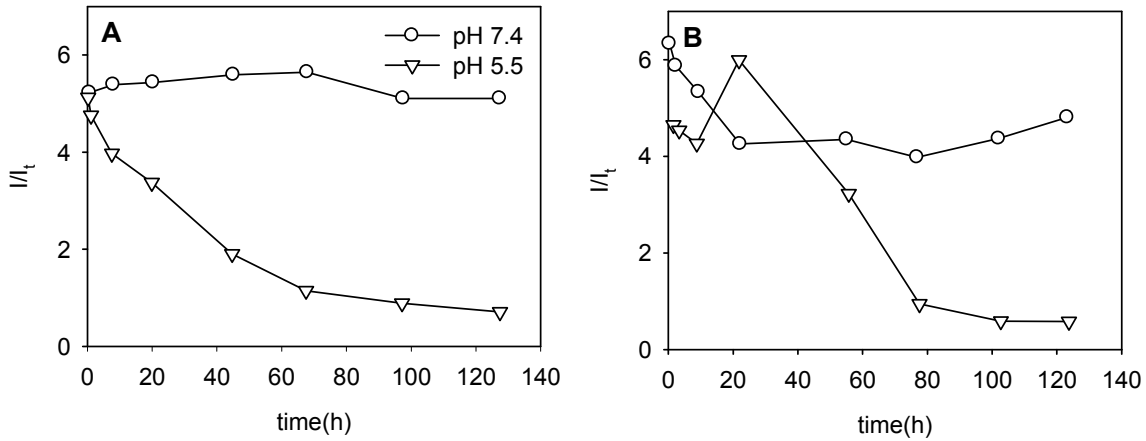


Figure S9. Time dependence of the intensity of DPPC/DPPG liposomes (60:40 m/m ratio) coated with A) W2K3, and B) W2R3 at different pHs in HBS. $\rho_{p/l} = 20$. Temperature = 37 °C.

For the liposome coated with W2K3, its behavior was similar to naked liposome at pH 7.4 (Figure S9A), suggesting that the coated liposomes were stable in solution of natural pH.

However, the scattered intensity sharply decreased to a level close to the intensity of solvent at pH 5.5 (Figure S9A). As the scattered intensity decreased, the size distribution remained constant at the beginning, and then became broad in 45 h (Figure S10A). A multimodal distribution was detected in 97 h. The size of the largest fragment was in the order of micrometer scale, indicating the occurrence of macrophase separation.

For the liposome coated with W2R3, its size distribution was broader than that of the naked liposome right after coating at pH 7.4, which was similar to that at $\rho_{p/l} = 1.0$. At pH 5.5, the scattered intensity exhibited a heavy fluctuation in the first 22 h, followed by a gradual decrease to a constant level (Figure S9B). Figure S10B shows that the particle sizes were constant at the first stage and then began to increase at 22 h, which accounted for the increase of the scattered

intensity shown in Figure S9B. The size distribution became narrow at this stage. Similarly, the decrease of the scattered intensity together with the gradual increase of the particle size suggested the heavy rupture of liposomes at pH 5.5 in the later stage.

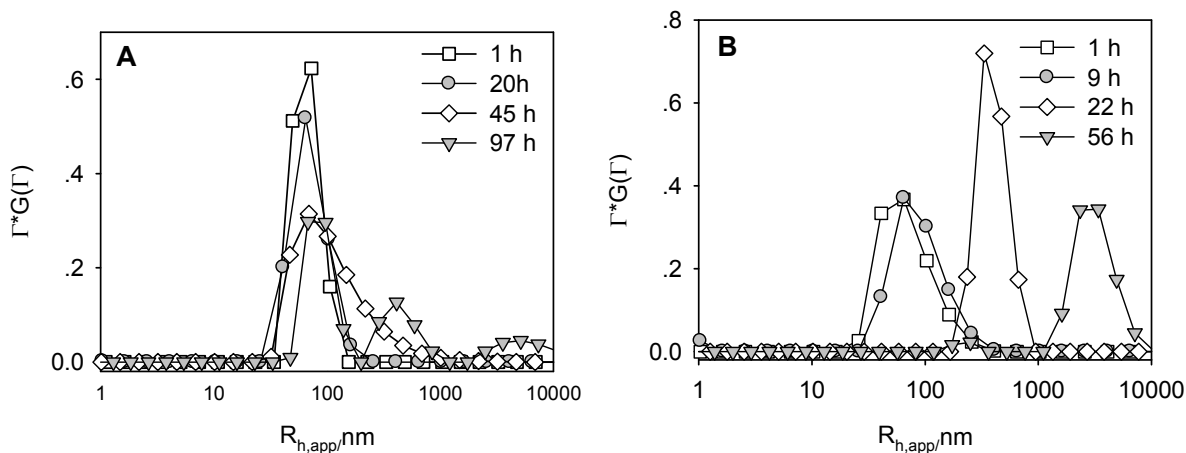


Figure S10. Size distribution of DPPC/DPPG liposomes (60:40 m/m ratio) coated with (A) W2K3, and (B) W2R3 at different time points at pH 5.5. Scattering angle: 30° . $\rho_{p/l} = 20$. Temperature = 37°C .

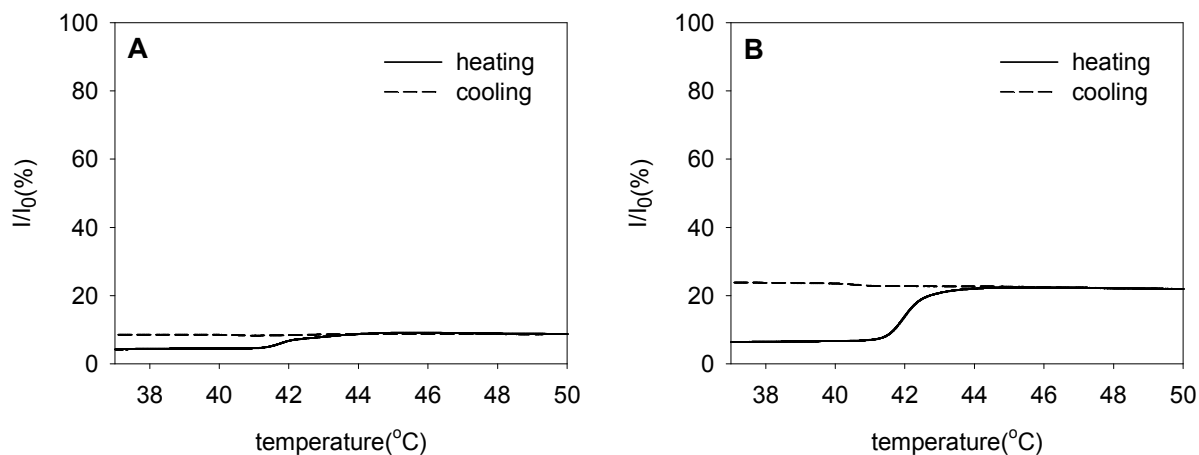


Figure S11. Temperature dependence of the fluorescence from uncoated DPPC/DPPG liposomes (60:40 m/m ratio) encapsulated with calcein at (A) pH 7.4, and (B) pH 5.5. $\rho_{p/l} = 1$. Heating rate: $0.1^\circ\text{C}/\text{min}$. Cooling rate: $0.2^\circ\text{C}/\text{min}$. $\lambda_{\text{ex}} = 490$ and $\lambda_{\text{em}} = 520$ nm.

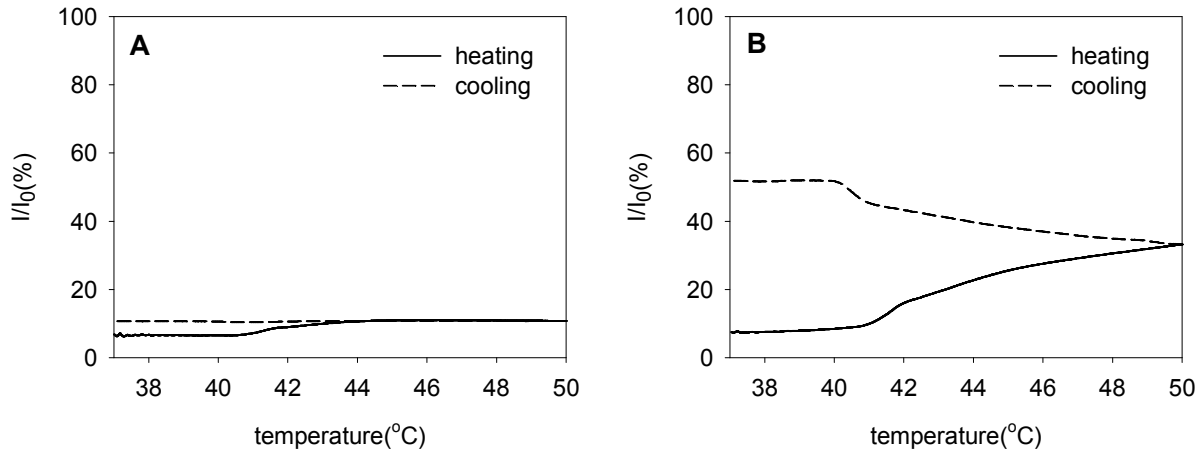


Figure S12. Temperature dependence of the fluorescence from W2R3 coated DPPC/DPPG liposomes (60:40 m/m ratio) encapsulated with calcein at (A) pH 7.4, and (B) pH 5.5. $\rho_{p/l} = 1$. Heating rate: 0.1 °C/min. Cooling rate: 0.2 °C/min. $\lambda_{ex} = 490$ and $\lambda_{em} = 520$ nm.

Giant Unilamellar Vesicles (GUV) with peptides

GUVs were prepared by electroformation method.^{1,2} The device was similar to that described by Angelova *et al.*³ The total lipid concentration was 3.75 mg/mL in 95% chloroform / 5% acetonitrile. The solution was spin-coated at 800 rpm for 1 minute onto the surface of a glass (50 mm x 50 mm x 1.1 mm) with a coating of conductive ITO⁴ The ITO coated glass was cleaned beforehand. The PDMS chamber between two ITO-glasses was 2 mm thick. The two glass slides were hold together with binder clips. After incubated at 50 °C for 10 min, the chamber was filled with 0.10 M sucrose solution (which was also heated to 50 °C) and immediately applied a 2.0 V (peak-to-peak), 10 Hz ac electric field using a function generator. After 4 hours, the formed GUVs were detached from the glass by applying a 3.0 V (peak-to-peak), 5 Hz ac field for 1 hour.

The GUVs were viewed by Nikon A1R-si Laser Scanning Confocal Microscope. 10 μL of GUV suspension in 0.10 M sucrose was added to 200 μL solution containing 3.0 μM peptide and 0.10 M glucose. Since the sucrose solution was denser than the glucose solution, GUVs will sink to the bottom of the chamber.

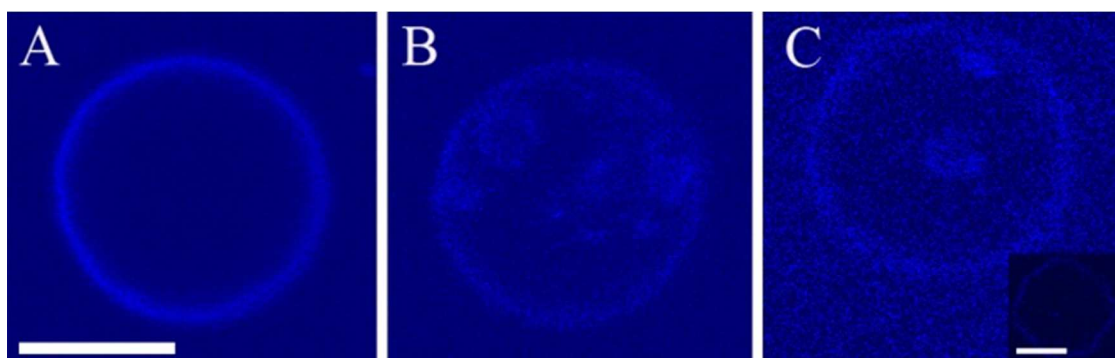


Figure S13. The GUV images of DPPC/DPPG (80:20 m/m ratio) with 0.1% perylene at 50 $^{\circ}\text{C}$ after added to A) buffer, B) W2K3, and C) W2R3. Scale bar: 10 μm .

The fluorescence intensities of non-charged dye (perylene) on the GUVs in Figure S13 became heterogeneous in the presence of peptides, indicating the occurrence of lipid demixing. As for W2R3 (Figure S13C), the deformation of vesicles (inset in Panel C) was also observed. Since perylene is not charged and buried inside the bilayer, it did not interact directly with the peptide. The redistribution of perylene was caused by the interaction between lipids and peptides.

References

1. M. Angelova, D. S. Dimitrov, *Progr. Colloid Polym. Sci.* **1988**, 76, 59-67.
2. T. Shimanouchi, H. Umakoshi, R. Kuboi, *Langmuir* **2009**, 25, 4835-4840.
3. M. Angelova, S. Soleau, P. Meleard, J.F. Faucon, P. Bothorel, *Prog. Colloid Polym. Sci.* **1992**, 89, 127.

4. Estes, D. J.; Mayer, M., Electroformation of giant liposomes from spin-coated films of lipids.
Colloids and Surfaces B: Biointerfaces **2005**, *42* (2), 115-123.